Organic & Biomolecular Chemistry

www.rsc.org/obc

Volume 10 | Number 18 | 14 May 2012 | Pages 3565–3768

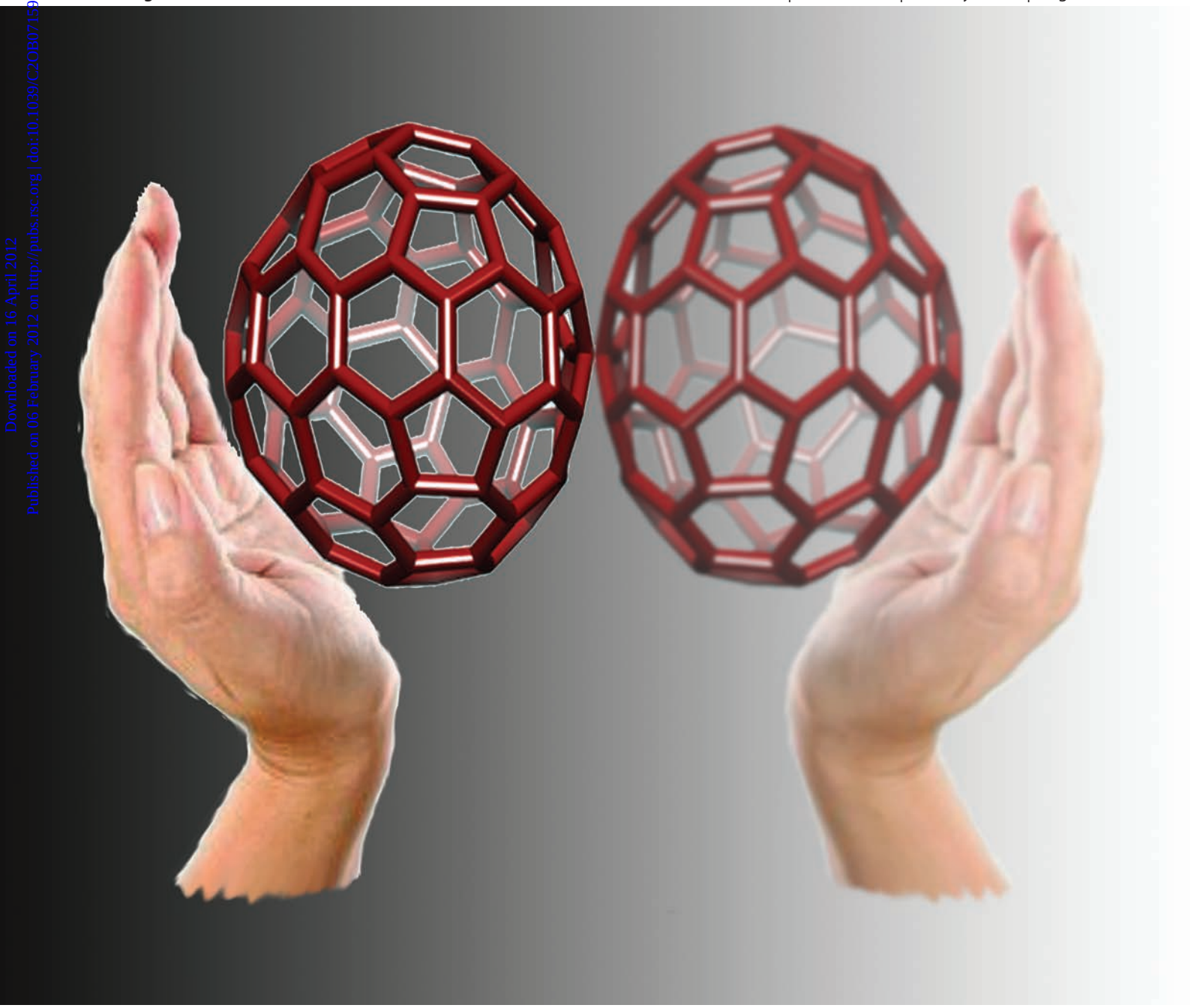

ISSN 1477-0520

RSC Publishing

EMERGING AREA
Emilio M. Pérez and Nazario Martín
Chiral recognition of carbon nanoforms

1477-0520(2012)10:18;1-C

Organic & Biomolecular Chemistry

Dynamic Article Links
View Online

Cite this: *Org. Biomol. Chem.*, 2012, **10**, 3577

www.rsc.org/obc

EMERGING AREA

Chiral recognition of carbon nanoforms

Emilio M. Pérez*[a] and Nazario Martín*[a,b]

Received 22nd December 2011, Accepted 6th February 2012
DOI: 10.1039/c2ob07159b

The selective recognition of chiral carbon nanoforms poses a fundamental challenge. New design principles must be devised to construct hosts capable of enantiodiscrimination between species in which chirality does not arise from asymmetric carbon atoms. In this emerging area article, we provide an overview of some of the relatively few successful examples of chiral recognition of carbon nanoforms, highlighting their common features with the aim of helping to develop general trends for the design of new generations of hosts.

Introduction

Chiral recognition is the study of the supramolecular interaction between chiral compounds. Its main aim is to obtain hosts capable of associating selectively a given isomer (often enantiomer) of a particular compound, habitually with the final objective of separating it from its optical antipode. Given the crucial importance of chirality in chemistry and biology, chiral recognition has been and continues to be one of the most active areas of supramolecular chemistry.

The design principles for the construction of enantioselective hosts for molecules in which chirality arises from one or more asymmetric carbon atoms were established several decades ago by Davankov, with his three point interaction model (Fig. 1).[1] In a very intuitive manner, the model predicts that at least three contact points are needed to discriminate between enantiomers.

Although it does not account for all cases of enantioselective recognition,[2] Davankov's model is as simple as it is useful… except for chiral molecules *without* asymmetric carbons!

[a]*Facultad de Ciencias Módulo C-IX, 3ª planta, Avda. Fco. Tomás y Valiente, 7 Ciudad Universitaria de Cantoblanco, 28049 Madrid, Spain. E-mail: emilio.perez@imdea.org*
[b]*Departamento de Química Orgánica, Facultad de Química, Universidad Complutense de Madrid, 28040, Spain. E-mail: nazmar@quim.ucm.es*

Emilio M. Pérez

Emilio M. Pérez obtained his BSc and MSc from the Universidad de Salamanca (Spain), under the supervision of Prof. Joaquín R. Morán. He then joined the group of Prof. David A. Leigh at the University of Edinburgh (UK) where he obtained his PhD in 2005. His PhD work was recognized with the 2006 IUPAC Prize for Young Chemists. He joined the group of Prof. Nazario Martin at Universidad Complutense de Madrid in 2005. In December 2008 he joined the IMDEA Nanoscience as a Ramón y Cajal researcher where he has received the 2009 RSEQ Prize for Novel Researchers and the 2010 UCM Foundation "Premio Joven" for Science and Technology. His main research interests concern molecular recognition, the self-assembly of functional materials and the construction of molecular machinery.

Nazario Martín

Nazario Martín is professor of Chemistry at Universidad Complutense and deputy-Director of IMDEA-Nanoscience. His research interests span a range of targets with emphasis on the covalent and supramolecular chemistry of carbon nanostructures in the context of new reactivity and chirality, electron transfer processes, photovoltaic applications and nanoscience. He is a member of the Editorial Board of Chemical Communications*, a member of the international advisory board of* The Journal of Organic Chemistry and ChemSusChem*, and the Regional Editor for Europe of* Fullerenes, Nanotubes and Carbon Nanostructures*. He is a member of the Real Academia de Doctores de España, a fellow of The Royal Society of Chemistry and former President of the Real Sociedad Española de Química (2006–2012).*

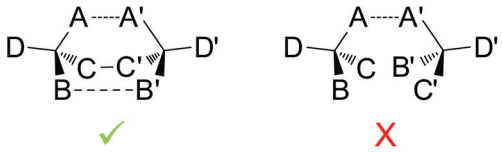

Fig. 1 Davankov's three point interaction model.

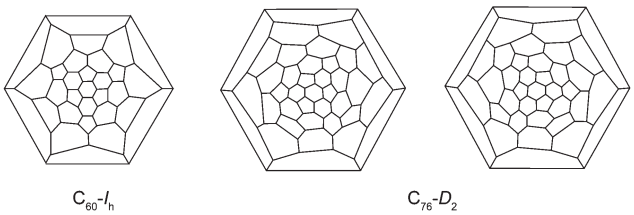

Fig. 2 Schlegel diagrams of the nonchiral C_{60}-I_h, and of the two enantiomers of the inherently chiral C_{76}-D_2.

Unfortunately, this is the case of the inherently chiral higher fullerenes and chiral carbon nanotubes. Our aim in this manuscript is to help establish general criteria to design hosts for the chiral recognition of these nanoforms of carbon. We will illustrate our considerations with a non-comprehensive overview of the successful examples reported to date. But first, let us begin with an overview of the origin and types of chirality in these molecular species.

Inherently chiral fullerenes

The term "inherent chirality" was first used by Böhm to refer to calix[4]arenes with an asymmetric substitution pattern in their upper rim and sufficiently bulky substituents in the lower rim to prevent cone inversion. Later, the term inherently chiral has been broadly applied to chiral molecules that do not fit into definitions of other types of chirality. Schiaffino[3] and Szumna[4] have defined inherent chirality as arising from the introduction of curvature in an ideal planar structure that is devoid of perpendicular symmetry planes in its bidimensional representation.

In the case of fullerenes, their bidimensional representations are the corresponding Schlegel diagrams. Therefore, the fullerenes with neither perpendicular symmetry axes nor planes in their Schlegel representations are inherently chiral (Fig. 2).

Although conceptually simple, constructing Schlegel diagrams of fullerenes is laborious and not always straightforward in practice, and becomes more complicated with increasing number of carbon atoms. Moreover, the inherently chiral fullerenes exist in several geometries (for example, C_{78} exists in D_3, C_{2v} and D_{3h} point group forms).

A more intuitive form of viewing chirality in fullerenes is helicity. From this point of view, C_{76} is doubly helical chiral. This is in fact how it was defined in the first theoretical[5] and experimental[6,7] descriptions of C_{76}. 3-D models of the two enantiomers of C_{76}-D_2 are shown in Fig. 3.

Chiral carbon nanotubes

Single wall carbon nanotubes (SWNTs) are allotropes of carbon with cylindrical structure. Their structure can be visualized as

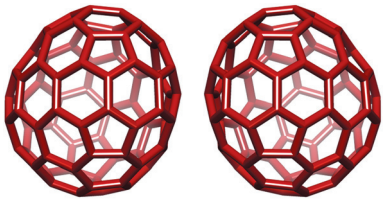

Fig. 3 Enantiomers of C_{76}-D_2.

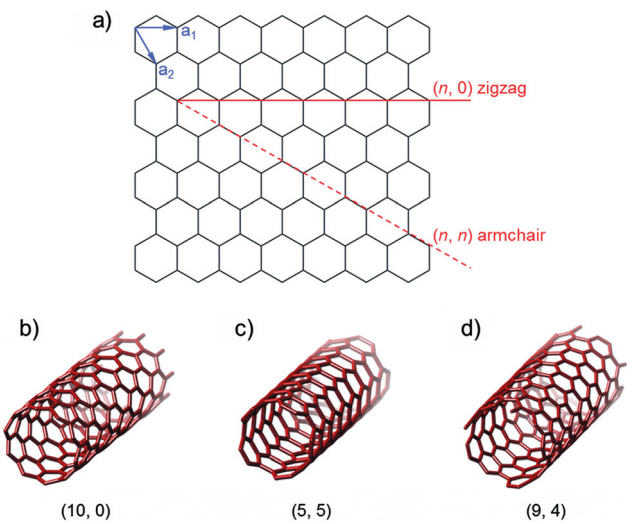

Fig. 4 (a) Formation of SWNTs from graphene; (b) a zigzag SWNT (10, 0); (c) an armchair SWNT (5, 5); (d) a chiral SWNT (9,4).

stemming from the wrapping of a layer of graphene to form a cylinder. The way that the graphene layer is folded is defined by a pair of indices (n, m), where n and m are integers denoting the number of unit vectors $\boldsymbol{a}_1$ and $\boldsymbol{a}_2$ along two directions at 60° to each other in the honeycomb structure of graphene (Fig. 4a). The line representing the sum of the vectors ($n\boldsymbol{a}_1 + m\boldsymbol{a}_2$) defines the circumference of the CNT along the plane perpendicular to its long axis. Nanotubes of the type (n, 0) are called zigzag SWNTs (red solid line in Fig. 4a and Fig. 4b). Nanotubes where $n = m$ are called armchair SWNTs (red dashed line in Fig. 4a and Fig. 4c). These two types of SWNTs are achiral, all other combinations of (n, m) give rise to chiral SWNTs. A 3D model of an example of each type of SWNT is shown in Fig. 4b–d. The helical nature of the chirality in SWNT is evident from observation of Fig. 4d.

A very important fact from the point of view of molecular recognition is that chirality and diameter in SWNTs are biunivocally related. The diameter of a SWNT of indices (n, m) is given by:

$$d(n,m) = 0.246/\pi \sqrt{(n^2 + nm + m^2)} \quad (1)$$

This means that, in theory, the problem of stereoselective recognition of SWNTs can be reduced to a problem of fine size/diameter selectivity. But there is one more level of complexity in chiral SWNTs: handedness. SWNTs with identical chiral indices can form P or M helices, which arise from folding of the graphene sheet from top to bottom or the other way around (see below).

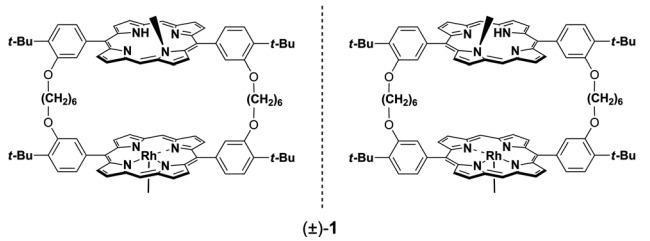

Fig. 5 Chemical structure of the chiral sensor reported by Aida *et al.*[12]

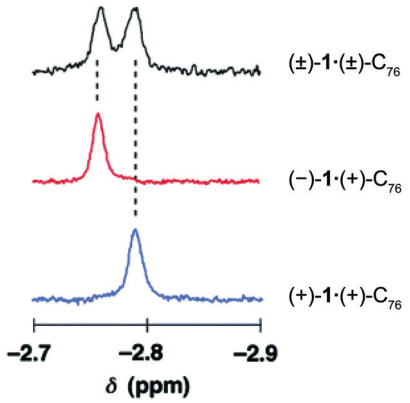

Fig. 6 ^{1}H NMR (500 MHz) spectra (NH signals of **1**) of equimolar mixtures of (+)-host/(+)-C_{76} (blue curves), (−)-host/(+)-C_{76} (red curves), and (±)-host/(±)-C_{76} (black curves) in toluene-d_8 at 20 °C. Reprinted with permission from ref. 12. Copyright 2006 American Chemical Society.

Enantioselective recognition of fullerenes

The supramolecular chemistry of C_{60} and C_{70} is very well developed. A plethora of receptors with varied binding abilities has been reported.[8–11] Given their structural similarities, the fundamental principles for the noncovalent binding of smaller (C_{60} and C_{70}) and higher (C_{76}, C_{78} and C_{84}) fullerenes should be identical. Consequently, the most immediate strategy for the design of enantioselective hosts for the higher fullerenes is the introduction of a chiral element into the structure of a previously known fullerene host. This was the approach that Shoji, Tashiro and Aida followed to construct the first chiral sensor for C_{76} (Fig. 5).[12]

They based their design on their remarkably successful series of bisporphyrin macrocyclic hosts for fullerenes.[10,13–17] In this case, they utilized a rhodium metalloporphyrin, which establishes strong noncovalent interactions with the fullerenes, and a distorted *N*-methylporphyrin as a source of chirality,[18] to produce (±)-**1**. Host (±)-**1** was shown to associate C_{76} through UV-vis titration experiments, showing a binding constant of log K_a = 7.2 in toluene at room temperature. Upon formation of the racemic complex, the porphyrin NH shows two distinctive ^{1}H NMR signals at δ = −2.76 and −2.79 ppm. With pure samples of (+)-**1** and (−)-**1** and enantiomerically enriched samples of (+)-C_{76} and (−)-C_{76} the authors demonstrated that each of those signals originated from a diastereomeric pair: (−)-**1**·(+)-C_{76}/(+)-**1**·(−)-C_{76} and (+)-**1**·(+)-C_{76}/(−)-**1**·(−)-C_{76} (Fig. 6).

Four years later, the same authors reported host **2**, capable of extracting C_{76} enantioselectively.[19] The structure of **2** (Fig. 7)

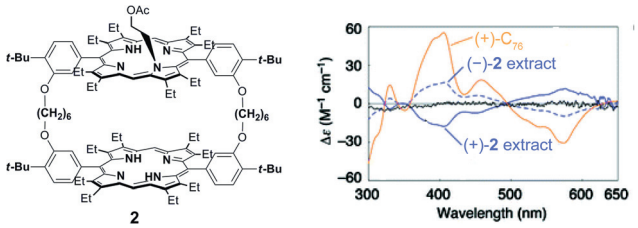

Fig. 7 Chemical structure of host **2** and CD spectra of C_{76} extracted with **2** (blue) along with that of an almost pure enantiomer of C_{76} (orange) as a reference. Adapted with permission from ref. 19. Copyright 2010 American Chemical Society.

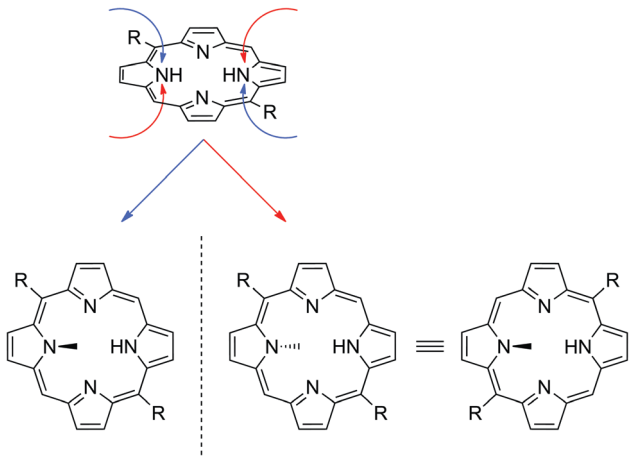

Fig. 8 Inherent chirality in *N*-methylporphyrins.

features two free-base porphyrins with ethyl substituents in the β-positions to augment π-basicity (*i.e.* increased electron density). In this case, the *N*-alkyl substituent is an acetoxyethyl moiety, which is more sterically demanding than the methyl group in **1**, and therefore introduces more distortion in the chiral part of the host. Mixing a 10-fold excess of (+)-**2** with (±)-C_{76} in toluene, produced a mixture of associates and free host, which was separated through size-exclusion chromatography. The fraction containing **2**·C_{76} was further subjected to column chromatography to separate the guest from the host. The resulting C_{76} was CD active, indicating that it had been enriched in (−)-C_{76}. When the same procedure was carried out with (+)-**2**, the opposite fullerene enantiomer was obtained. Comparing the $\Delta\varepsilon$ of the extract with that of enantiomerically pure C_{76}, the authors estimated a modest enantiomeric excess of 7%.

Are there any general conclusions to be extracted from these two successful examples? Is the introduction of any type of chiral element in a host for C_{76} sufficient to induce enantioselectivity? *N*-alkylporphyrins are chiral due to the deviation of planarity caused by the steric impediment of the alkyl substituent. The enantiomeric pair arises from alkylation from above or below the mean plane of the porphyrin. For porphyrins with two *meso* substituents, like those in **1** and **2**, this is equivalent to changing the arrangement of the peripheral substituents (Fig. 8), exactly like in the case of the inherently chiral calix[4]arenes. The 2-D projection of the *N*-alkylporphyrin has no perpendicular symmetry axes or planes, that is, *N*-alkyl porphyrins are inherently chiral: they show the same type of chirality of C_{76}.

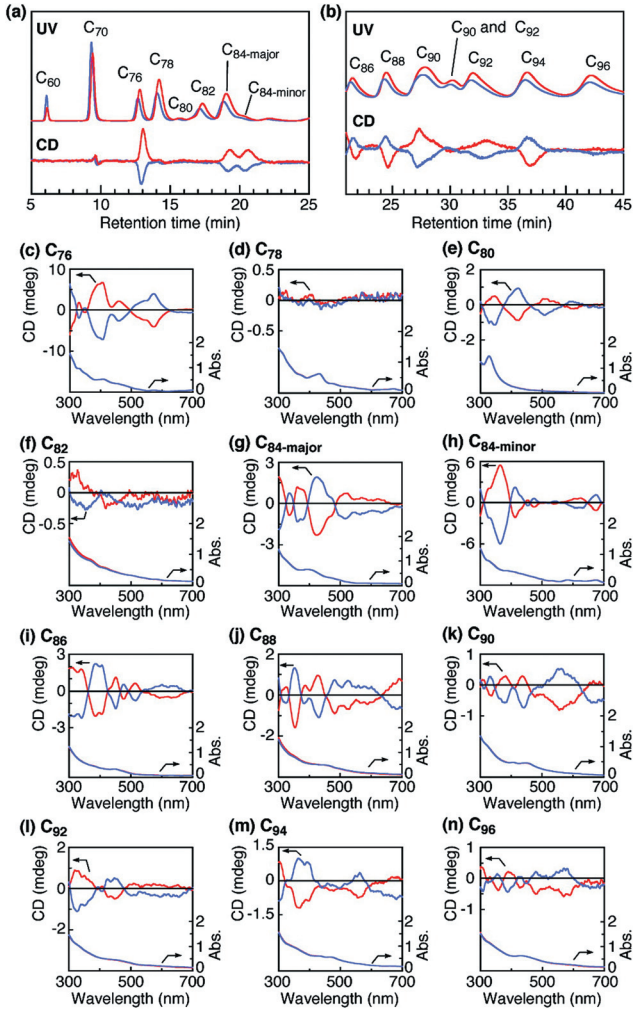

Fig. 9 (a, b) UV (356 nm, top) and CD (375 nm, bottom) detected HPLC chromatograms of the extracted fullerenes from carbon soot using optically active helical st-PMMAs prepared with (*R*)-1-phenylethylamine (red lines) and (*S*)-1-phenylethylamine (blue lines) as solvent. CD (top) and absorption (bottom) spectra of fractionated (c) C_{76}, (d) C_{78}, (e) C_{80}, (f) C_{82}, (g) $C_{84\text{-major}}$, (h) $C_{84\text{-minor}}$, (i) C_{86}, (j) C_{88}, (k) C_{90}, (l) C_{92}, (m) C_{94}, and (n) C_{96} measured in *o*-dichlorobenzene at 25 °C. Reprinted with permission from ref. 21. Copyright 2010 American Chemical Society.

Besides small-molecule hosts, a different approach to the enantiomeric resolution of C_{76} is the use of macromolecules. For example, Okamoto and co-workers reported a method to obtain optically active C_{76} through iterative high-performance liquid chromatography (HPLC) utilizing a chiral stationary phase based on amylose tris(3,5-dimethylphenylcarbamate).[20]

More recently, the groups of Kawauchi and Yashima have utilized a syndiotactic poly(methyl methacrylate) (st-PMMA) to extract fullerenes in a selective manner.[21] Remarkably, their method shows a nearly perfect C_{70} over C_{60} selectivity, and even more impressively, it could be used to obtain optically active samples of C_{76}, C_{80}, C_{84}, C_{86}, C_{88}, C_{90}, C_{92}, C_{94} and C_{96}! (Fig. 9). Although the enantiomeric excesses were estimated to be low (*ca.* 4%), this is so far the most versatile method for the resolution of the higher fullerenes.

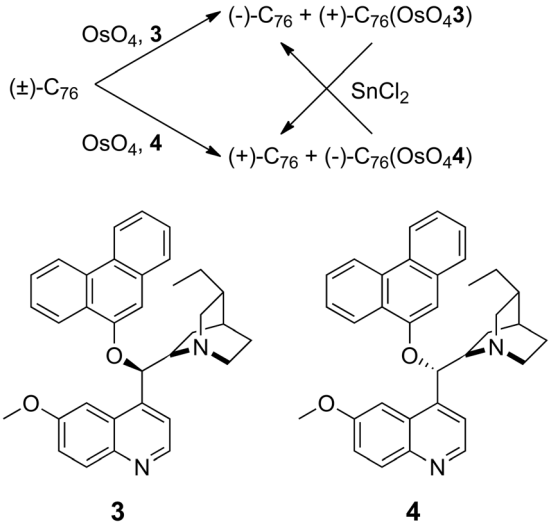

Fig. 10 Scheme for the kinetic resolution of C_{76} by selective osmylation-reduction, and structure of the *cinchona*-based catalysts.

Although understanding the reason behind the recognition process for these macromolecules is not as intuitive as for small-molecule hosts, one common aspect immediately stands out: both amylose and st-PMMA feature helical chirality. Again, this matches the type of chirality of the fullerene guests.

So, when designing enantioselective hosts for the higher fullerenes, is it a prerequisite to utilize inherently or helically chiral recognition motifs? Unfortunately, the literature reports are still insufficient to arrive at a solid final conclusion, nevertheless, the few successful examples reported to date do point in that direction.

Other types of chiral elements have been introduced in fullerene hosts, presumably with the final aim of obtaining enantioselectivity towards the chiral fullerenes. For example, in 2010 Pasini and co-workers reported the synthesis of a series of enantiomerically pure chiral macrocycles based on the axially chiral 1,1′-binaphthyl-2,2′-diol (BINOL).[22,23] Surprisingly, the authors only reported on the association of the nonchiral C_{60} despite the chiral structure of their hosts.

An exception to this trend was the first kinetic resolution of C_{76}, reported by Hawkins and Meyer in 1993.[7] They performed an enantioselective osmylation–reduction protocol on C_{76} as shown in Fig. 10, catalyzed by the pseudoenantiomeric ligands **3** and **4**. When rationalizing their results, the authors noted that "chiral recognition may involve diastereotopic attractive π–π interactions between the phenanthryl units of **3** and **4** and the contoured fullerene surfaces." However, the resolution occurs under kinetic control, unlike standard molecular recognition events, which take place under thermodynamic equilibrium conditions.

Chiral recognition of SWNTs

The chiral indices of SWNTs determine their chirality, diameter, and electronic properties. Although methods for the selective synthesis of a particular type of SWNTs have been reported,[24,25] most samples of SWNTs are composed of a complicated mixture of nanotubes. The separation of SWNTs according to their

chirality is a phenomenal challenge from both the fundamental and applied point of view. The separation of metal from semiconductor SWNT based on their diameters was achieved through density gradient ultracentrifugation (DGU).[26,27] Likewise, the different affinity of octadecylamine for metallic and semiconducting nanotubes has been used to separate them through a dispersion–centrifugation process,[28] and also through sedimentation from a THF suspension.[29]

A more challenging problem is to differentiate between SWNT of similar diameter and electronic properties but different chirality. For instance (9, 1) and (6, 5) SWNTs show the same diameter of 0.75 nm, and are both semiconducting. So far, two lines of research have produced the most successful results towards the chiral recognition of SWNTs:[30–32] one approach is based on the interaction between metalloporphyrin molecular tweezers and nanotubes,[33] and another one exploits the wrapping of single strand DNA (ssDNA) around SWNTs.[34]

Starting with the latter, all four nitrogenous bases in DNA show strong π–π interactions with graphitic surfaces. Making use of *in vitro* evolution techniques borrowed from molecular biology, Zheng and co-workers found ssDNA sequences that bound to SWNTs with affinities comparable with the nanotube–nanotube interactions, which allowed them to disperse the ssDNA–SWNT hybrids in water.[35] Later, a more thorough screening of the ssDNA library led to the identification of a sequence, namely alternating dC (deoxycytidylate) and dT (deoxythymidylate), or $d(CT)_n$ where n = 10–45, produced separation of the ssDNA–SWNT hybrids upon subjecting the mixture to ion exchange chromatography (IEX).[36] The vis-NIR spectra of the fractionated ssDNA–SWNT hybrids are shown in Fig. 11.

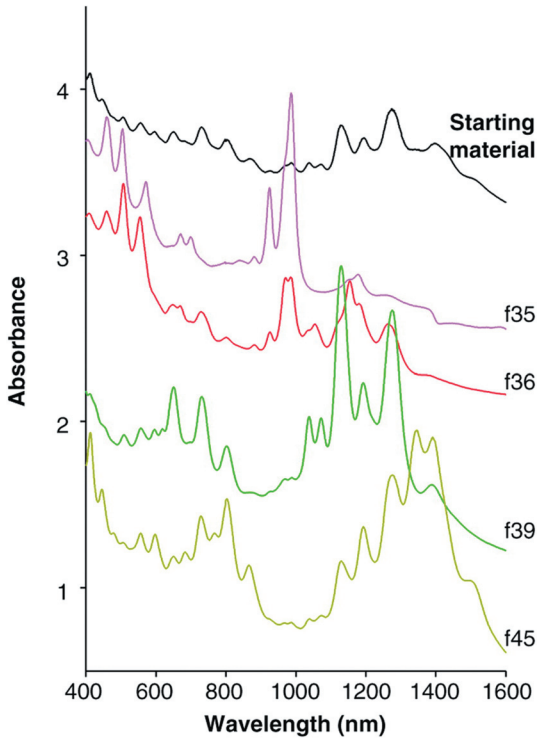

Fig. 11 Absorption spectroscopy on fractionated SWNTs. Absorption spectra of the starting material (black), f35 (pink) (4×), f36 (red), f39 (green) (0.5×), and f45 (olive green). Reprinted with permission from ref. 36. Copyright 2003 American Association for the Advancement of Science.

The spectra clearly show evidence for structure-based SWNT separation. The starting material shows a spectrum typical of dispersed SWNTs in aqueous solution, with multiple peaks arising from different types of tubes overlapping across the entire spectrum. In contrast, the spectrum of f35 is dominated by one major peak in the S_{11} region, at 980 nm, which was assigned to the S_{11} transition from the smallest diameter semiconducting tubes found in HiPco nanotubes. Besides this absorption, M_{11} transitions gain in relative absorbance compared to the starting material, indicating enrichment in metallic tubes. The S_{11} region from later fractions (f36, f39, and f45) shows a systematic red-shift of intensity, which is indicative of a gradual increase in average semiconducting tube diameter. This is accompanied by a simultaneous decrease of absorbance in the M_{11} region, corresponding to a depletion of metallic tubes. Moreover, based on Raman spectroscopy, which provides a direct measurement of the nanotubes' diameter, the authors concluded that up to 29 different types of SWNTs could be resolved.

By performing size exclusion chromatography (SEC) prior to IEX, the resolution of this technique could be pushed to separate single chirality tubes, even in cases where the nanotubes show identical diameter, like (9, 1) and (6, 5).[37] This improvement was attributed to homogenization of the sample in terms of SWNT length.

Finally, the Dupont scientists achieved the ultimate selectivity, separating all 12 major single-chirality SWNTs present in commercial HiPco tubes.[38] To realize such an amazing accomplishment, Zheng's team screened a library of ~10^{60} ssDNA sequences, and identified specific sequences for each type of chiral SWNT. By careful tuning of the experimental conditions, including different salts, and incubation periods, single-chirality SWNTs in high purity (60–90%) were obtained. This is evidenced in their vis-NIR spectra (Fig. 12).

The extreme selectivity of the ssDNA method, capable of separating single-chirality SWNTs, leaves only one more degree of complexity to be addressed, that is, handedness. Chiral nanotubes come as enantiomeric pairs of *P* and *M* helices (Fig. 13a). The separation of enantiomers within one specific type of chiral SWNT is the ultimate challenge in the chiral recognition of SWNTs. The selective extraction of optically active nanotubes was achieved by the team of Komatsu, utilizing the chiral bisporphyrin tweezers shown in Fig. 13b.[39–42]

The rigid structure of the porphyrin tweezers allows them to discriminate between nanotubes of different chiral indices (*i.e.* diameter) while the addition of chiral centres at the substituents of the porphyrins make them selective between enantiomers of single-chirality SWNTs. The net result is that upon extraction of a methanol suspension of a commercial sample of CoMoCAT with, for instance, (*R*)-**7** and (*S*)-**7**, followed by centrifugation and removal of the host molecules, there is a considerable enrichment in opposite enantiomers of the (6, 5) SWNT, as demonstrated through CD measurements (Fig. 14).[42] Comparing with results obtained from nonlinear DGU,[43] the authors estimated a remarkable 67% ee.

Tweezers **8** show preference for (7, 4) SWNTs, while both **5** and **6** are selective towards (6, 5) nanotubes. Presumably, the

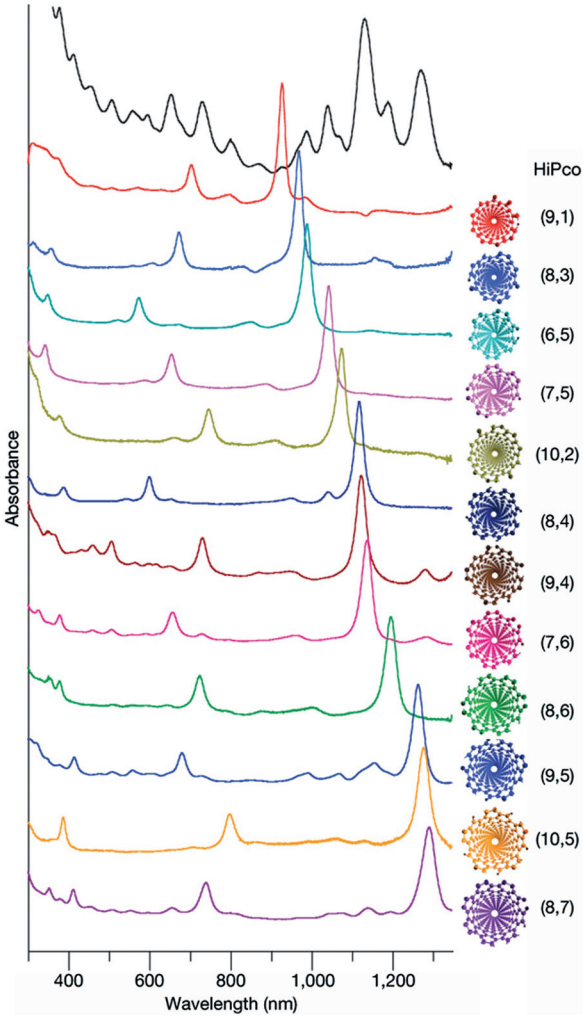

Fig. 12 Electronic absorption spectra of 12 purified semiconducting SWNTs (ranked according to the measured E_{11} absorption wavelength) and the starting HiPco mixture. Reprinted with permission from ref. 38. Copyright 2009 Nature Publishing Group.

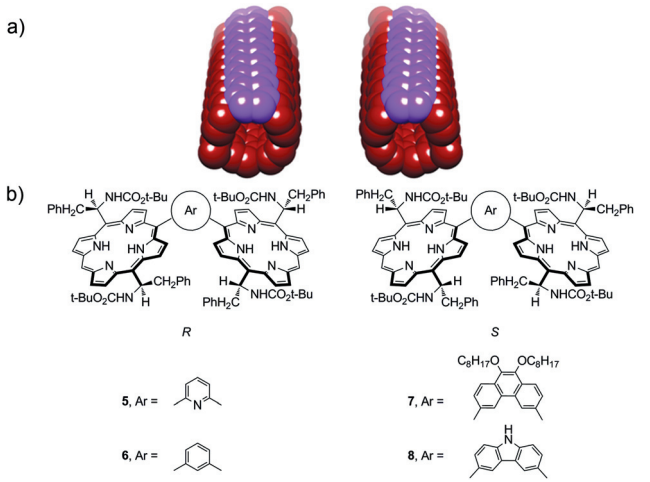

Fig. 13 (a) *M* and *P* (6, 5) SWNTs. (b) Chemical structures of the chiral bisporphyrin tweezers reported by Komatsu and co-workers.[39–42]

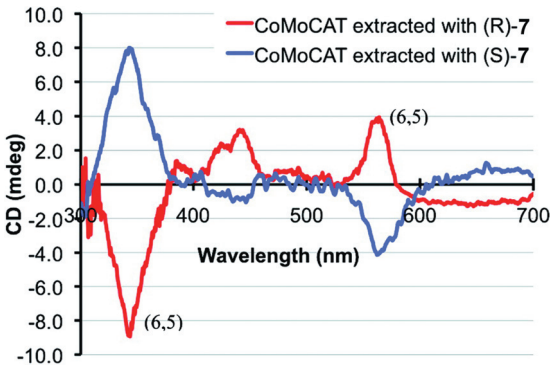

Fig. 14 CD spectra of SWNTs extracted with (*R*)- and (*S*)-**7**. Reprinted with permission from ref. 42. Copyright 2010 American Chemical Society.

screening of a larger collection of aromatic spacers, and/or chiral substituents will eventually lead to tweezers selective for any given chiral nanotube.

In the case of SWNTs, there are no definitive trends in the design for chiral hosts. While helically chiral polymers have shown some of the most impressive results, the small-molecule porphyrin tweezers reported by Komatsu do not show helical chirality, yet they are able to perform extractions of SWNTs with both diameter and handedness selectivity. In this particular case, the origin of the enantioselectivity is unclear, at least to us. It is also surprising that they have not been applied to the enantioselective recognition of the inherently chiral higher fullerenes.

Conclusions

The chiral recognition of carbon nanoforms represents a genuine challenge from the fundamental point of view. While the principles for the enantioselective recognition of molecules in which chirality arises from asymmetric carbon atoms are well established,[1] intuitive and of general applicability, there are no such general design guidelines for the construction of enantioselective hosts for the inherently chiral fullerenes, or for SWNTs. In the case of SWNTs, their chiral recognition has profound practical implications, since their electronic properties depend directly on their chirality.

In this emerging area article, we have given an overview of some of the relatively few successful examples of chiral recognition of fullerenes and SWNTs[44] reported to date. Besides the mere scientific account, our intention was to draw some general guidelines that we hope will be useful to continue to advance in this field. In this regard, here are our main conclusions:

(1) Small-molecule enantioselective hosts for fullerenes are based on designs that have already proved successful for the recognition of smaller fullerenes (C_{60} and C_{70}).

(2) Successful enantioselective hosts for the chiral fullerenes feature either inherently (small-molecule hosts) or helically chiral (macromolecule) recognition motifs. In this respect, it is worth noting that there are multiple inherently chiral molecules that might serve as scaffolds for the construction of enantioselective hosts and have not yet been tested.

(3) The selective recognition of SWNTs according to their chiral indices can in most cases be reduced to a problem of fine size/diameter selectivity. In this sense, rigid molecular hosts seem more suitable than flexible ones.

(4) Helically chiral macromolecules, like ssDNA or aromatic polymers,[44] have proven particularly successful for the chiral recognition of SWNTs.

All these observations come with a *caveat*: the number of reports on chiral hosts for either fullerenes or SWNTs is still relatively small. Much more information is required—hopefully on both successful *and* unsuccessful designs!—before definitive general design principles can be drawn.

Acknowledgements

Financial support from MICINN (CTQ2011-25714) is gratefully acknowledged. EMP is also thankful for a Ramón y Cajal Fellowship, co-financed by European Social Funds.

Notes and references

1 V. A. Davankov, *Chromatographia*, 1989, **27**, 475–482.
2 C. Fraschetti, M. Pierini, C. Villani, F. Gasparrini, S. L. Mortera, A. Filippi and M. Speranza, *Chem.–Eur. J.*, 2011, **17**, 3078–3081.
3 A. Dalla Cort, L. Mandolini, C. Pasquini and L. Schiaffino, *New J. Chem.*, 2004, **28**, 1198–1199.
4 A. Szumna, *Chem. Soc. Rev.*, 2010, **39**, 4274–4285.
5 P. W. Fowler, R. C. Batten and D. E. Manolopoulos, *J. Chem. Soc., Faraday Trans.*, 1991, **87**, 3103–3104.
6 R. Ettl, I. Chao, F. Diederich and R. L. Whetten, *Nature*, 1991, **353**, 149–153.
7 J. M. Hawkins and A. Meyer, *Science*, 1993, **260**, 1918–1920.
8 D. Canevet, E. M. Pérez and N. Martín, *Angew. Chem., Int. Ed.*, 2011, **50**, 9248–9259.
9 E. M. Pérez and N. Martín, *Chem. Soc. Rev.*, 2008, **37**, 1512–1519.
10 K. Tashiro and T. Aida, *Chem. Soc. Rev.*, 2007, **36**, 189–197.
11 T. Kawase and H. Kurata, *Chem. Rev.*, 2006, **106**, 5250–5273.
12 Y. Shoji, K. Tashiro and T. Aida, *J. Am. Chem. Soc.*, 2006, **128**, 10690–10691.
13 K. Tashiro, T. Aida, J.-Y. Zheng, K. Kinbara, K. Saigo, S. Sakamoto and K. Yamaguchi, *J. Am. Chem. Soc.*, 1999, **121**, 9477–9478.
14 J.-Y. Zheng, K. Tashiro, Y. Hirabayashi, K. Kinbara, K. Saigo, T. Aida, S. Sakamoto and K. Yamaguchi, *Angew. Chem., Int. Ed.*, 2001, **40**, 1857–1861.
15 Y. Shoji, K. Tashiro and T. Aida, *J. Am. Chem. Soc.*, 2004, **126**, 6570–6571.
16 A. Ouchi, K. Tashiro, K. Yamaguchi, T. Tsuchiya, T. Akasaka and T. Aida, *Angew. Chem., Int. Ed.*, 2006, **45**, 3542–3546.
17 M. Yanagisawa, K. Tashiro, M. Yamasaki and T. Aida, *J. Am. Chem. Soc.*, 2007, **129**, 11912–11913.
18 H. Kubo, T. Aida, S. Inoue and Y. Okamoto, *J. Chem. Soc., Chem. Commun.*, 1988, 1015–1017.
19 Y. Shoji, K. Tashiro and T. Aida, *J. Am. Chem. Soc.*, 2010, **132**, 5928–5929.
20 C. Yamamoto, T. Hayashi, Y. Okamoto, S. Ohkubo and T. Kato, *Chem. Commun.*, 2001, 925–926.
21 T. Kawauchi, A. Kitaura, M. Kawauchi, T. Takeichi, J. Kumaki, H. Iida and E. Yashima, *J. Am. Chem. Soc.*, 2010, **132**, 12191–12193.
22 C. Coluccini, D. Dondi, M. Caricato, A. Taglietti, M. Boiocchi and D. Pasini, *Org. Biomol. Chem.*, 2010, **8**, 1640–1649.
23 M. Caricato, C. Coluccini, D. Dondi, D. A. Vander Griend and D. Pasini, *Org. Biomol. Chem.*, 2010, **8**, 3272–3280.
24 M. C. Hersam, *Nat. Nanotechnol.*, 2008, **3**, 387–394.
25 X. Li, X. Tu, S. Zaric, K. Welsher, W. S. Seo, W. Zhao and H. Dai, *J. Am. Chem. Soc.*, 2007, **129**, 15770–15771.
26 M. S. Arnold, A. A. Green, J. F. Hulvat, S. I. Stupp and M. C. Hersam, *Nat. Nanotechnol.*, 2006, **1**, 60–65.
27 M. S. Arnold, S. I. Stupp and M. C. Hersam, *Nano Lett.*, 2005, **5**, 713–718.
28 Y. Maeda, S. Kimura, M. Kanda, Y. Hirashima, T. Hasegawa, T. Wakahara, Y. Lian, T. Nakahodo, T. Tsuchiya, T. Akasaka, J. Lu, X. Zhang, Z. Gao, Y. Yu, S. Nagase, S. Kazaoui, N. Minami, T. Shimizu, H. Tokumoto and R. Saito, *J. Am. Chem. Soc.*, 2005, **127**, 10287–10290.
29 D. Chattopadhyay, I. Galeska and F. Papadimitrakopoulos, *J. Am. Chem. Soc.*, 2003, **125**, 3370–3375.
30 For a method based on helical assemblies of flavin mononucleotide, see: S.-Y. Ju, J. Doll, I. Sharma and F. Papadimitrakopoulos, *Nat. Nanotechnol.*, 2008, **3**, 356–362.
31 For a method based on polyaromatic amphiphiles, see: R. Marquis, C. Greco, I. Sadokierska, S. Lebedkin, M. M. Kappes, T. Michel, L. Alvarez, J.-L. Sauvajol, S. p. Meunier and C. Mioskowski, *Nano Lett.*, 2008, **8**, 1830–1835.
32 For a method based on aromatic polymers, see: A. Nish, J.-Y. Hwang, J. Doig and R. J. Nicholas, *Nat. Nanotechnol.*, 2007, **2**, 640–646.
33 For a review, see: X. Peng, F. Wang, A. K. Bauri, A. F. M. M. Rahman and N. Komatsu, *Chem. Lett.*, 2010, **39**, 1022–1027.
34 For a review, see: X. Tu and M. Zheng, *Nano Res.*, 2008, **1**, 185–194.
35 M. Zheng, A. Jagota, E. D. Semke, B. A. Diner, R. S. McLean, S. R. Lustig, R. E. Richardson and N. G. Tassi, *Nat. Mater.*, 2003, **2**, 338–342.
36 M. Zheng, A. Jagota, M. S. Strano, A. P. Santos, P. Barone, S. G. Chou, B. A. Diner, M. S. Dresselhaus, R. S. McLean, G. B. Onoa, G. G. Samsonidze, E. D. Semke, M. Usrey and D. J. Walls, *Science*, 2003, **302**, 1545–1548.
37 M. Zheng and E. D. Semke, *J. Am. Chem. Soc.*, 2007, **129**, 6084–6085.
38 X. Tu, S. Manohar, A. Jagota and M. Zheng, *Nature*, 2009, **460**, 250–253.
39 X. Peng, N. Komatsu, S. Bhattacharya, T. Shimawaki, S. Aonuma, T. Kimura and A. Osuka, *Nat. Nanotechnol.*, 2007, **2**, 361–365.
40 X. Peng, N. Komatsu, T. Kimura and A. Osuka, *J. Am. Chem. Soc.*, 2007, **129**, 15947–15953.
41 X. Peng, N. Komatsu, T. Kimura and A. Osuka, *ACS Nano*, 2008, **2**, 2045–2050.
42 F. Wang, K. Matsuda, A. F. M. M. Rahman, X. Peng, T. Kimura and N. Komatsu, *J. Am. Chem. Soc.*, 2010, **132**, 10876–10881.
43 S. Ghosh, S. M. Bachilo and R. B. Weisman, *Nat. Nanotechnol.*, 2010, **5**, 443–450.
44 For a comprehensive review, see: N. Komatsu and F. Wang, *Materials*, 2010, **3**, 3818–3844.